

Portland State University

PDXScholar

Dissertations and Theses

Dissertations and Theses

1-1-2011

Polymer-Based Photoactive Surface for the Efficient Immobilization of Nanoparticles, Polymers, Graphene and Carbohydrates

Jing Yuwen

Portland State University

Follow this and additional works at: https://pdxscholar.library.pdx.edu/open_access_etds

Let us know how access to this document benefits you.

Recommended Citation

Yuwen, Jing, "Polymer-Based Photoactive Surface for the Efficient Immobilization of Nanoparticles, Polymers, Graphene and Carbohydrates" (2011). *Dissertations and Theses*. Paper 413.

<https://doi.org/10.15760/etd.413>

This Thesis is brought to you for free and open access. It has been accepted for inclusion in Dissertations and Theses by an authorized administrator of PDXScholar. Please contact us if we can make this document more accessible: pdxscholar@pdx.edu.

Polymer-Based Photoactive Surface for the Efficient Immobilization of
Nanoparticles, Polymers, Graphene and Carbohydrates

by

Jing Yuwen

A thesis submitted in partial fulfillment of the
requirements for the degree of

Master of Science
in
Chemistry

Thesis Committee:
Mingdi Yan, Chair
Andrea Mitchell Goforth
Shankar B. Rananavare

Portland State University
©2011

ABSTRACT

This thesis focuses on developing a new photocoupling surface, base on polyallylamine (PAAm), to increase the efficiency of the photocoupling agent perfluorophenyl azide (PFPA) in the immobilization of nanoparticles, carbohydrates and graphene. Extensive studies have been carried out in our lab on the covalent immobilization of polymers and graphene using PFPA-functionalized surfaces. Here we show that PAAm-based PFPA surface can be used to efficiently immobilize not only graphene and polymers but also nanomaterials and small molecules.

This was accomplished by first silanizing silicon wafers with PFPA-silane followed by attaching a thin film of PAAm by UV radiation. Treating the PAAm surface with *N*-hydroxysuccinimide-derivatized PFPA (PFPA-NHS) yielded the PAAm-PFPA surface. The functionalized surfaces were characterized by ellipsometry (layer thickness), contact angle (surface tension), and ATR-FTIR. The PAAm surface was further characterized by determining the density of amino groups on the surface.

The PAAm-PFPA surfaces were subsequently used to covalently immobilize polymers, nanomaterials, carbohydrates and graphene by a simple procedure of coating the molecules or materials on the PAAm-PFPA surface followed by UV irradiation. The resulting surfaces were characterized using ellipsometry, AFM, optical microscopy. The attached carbohydrates were further evaluated using lectins, i.e., carbohydrate-binding proteins.

ACKNOWLEDGEMENTS

I would like to express my appreciation to my advisor Dr. Mingdi Yan for her advice, expertise, guidance and patience during this research. Thanks to Dr. Andrea Mitchell Goforth and her group members for their kind help on the ATR-FTIR and DLS instruments. A special thanks to the members of the Yan research group for all their help and suggestions.

TABLE OF CONTENTS

ABSTRACT.....	i
ACKNOWLEDGEMENTS.....	ii
LIST OF TABLES.....	v
LIST OF FIGURES.....	vi
LIST OF SCHEMES.....	vii
LIST OF ABBREVIATIONS.....	viii
SECTION	
1. INTRODUCTION.....	1
2. EXPERIMENTAL.....	9
2.1 Materials.....	9
2.2 Instrumentation.....	10
2.3 Synthesis of PFPA-NHS.....	11
2.4 Synthesis of PFPA-silane.....	11
2.5 Preparation of PAAm-PFPA surface via PFPA.....	11
2.6 Preparation of Epoxy-PAAm-PFPA surface.....	12
2.7 Determination of amine density of PFPA-PAAm surface by UV-vis spectrometry.....	13
2.8 Preparation of glyco-nanoparticles.....	15
2.9 Immobilization of polymers.....	16

2.10 Immobilization of nanoparticles.....	16
2.11 Immobilization of graphene.....	17
2.12 Immobilization of carbohydrate.....	17
3. RESULTS AND DISCUSSION.....	19
3.1 Preparation of PAAm-PFPA surface via PFPA.....	19
3.2 Amino density determination of the PAAm surface.....	24
3.3 Preparation of PAAm-PFPA from epoxy surface.....	27
3.4 Immobilization of polymers.....	29
3.5 Immobilization of nanoparticles.....	31
3.6 Immobilization of graphene.....	36
3.7 Immobilization of carbohydrates.....	38
4. CONCLUSION.....	40
5. REFERENCES.....	42

LIST OF TABLES

1. Table 3.1 Surface concentration of amino groups on PAAm and PFPA-silane functionalized surfaces.....	26
--	----

LIST OF FIGURES

1. Figure 3.1 The thickness of different surface layers.....	20
2. Figure 3.2 IR of bulk PAAm•HCl, ATR-IR spectra of PAAm•HCl on PFPA, PAAm and PAAm-PFPA surface.....	24
3. Figure 3.3 Standard calibration curve of 4-nitrobenzaldehyde by measuring the maximal UV-Vis absorbance at 267 nm against its concentration.....	25
4. Figure 3.4 The thickness of different layers of Epoxy-PAAm-PFPA surface...	28
5. Figure 3.5 ATR-IR spectra of PAAm and PAAm-PFPA surfaces fabricated on epoxy surface.....	29
6. Figure 3.6 The thickness of PS and PEOX immobilized on different surfaces.....	30
7. Figure 3.7 DLS data of glyco-nanoparticles and AFM images of immobilization nanoparticles on PFPA-silane and PAAm-PFPA surfaces.....	36
8. Figure 3.8 Optical images of graphene solution on PFPA-silane and PAAm- PFPA surfaces.....	37
9. Figure 3.9 Fluorescence images of immobilized Man2 on PFPA-silane and PAAm-PFPA surfaces.....	39

LIST OF SCHEMES

1. Scheme 1.1 SAMs are formed by simply immersing a substrate into a solution of the surface-active molecule.....	3
2. Scheme 1.2 CH, NH insertion, and C=C addition reaction of PFPA.....	5
3. Scheme 1.3 Photo immobilization on PFPA surface.....	5
4. Scheme 1.4 Three different approaches for making PAAm-PFPA surfaces.....	8
5. Scheme 2.1 Determination of surface amine density by forming imine and releasing 4-nitrobenzaldehyde.....	14

LIST OF ABBREVIATIONS

AFM Atomic Force Microscopy

Con A Concanavalin A

DMF Dimethylformamide

FITC Fluorescein isothiocyanate

ATR-FTIR Attenuated Total Reflectance Fourier Transform Infrared
Spectroscopy

Man Mannose

NHS *N*-Hydroxysuccinimide

NMR Nuclear Magnetic Resonance Spectroscopy

PAAm Polyallylamine

PEOX Poly (2-ethyl-2-oxazoline)

PFPA Perfluorophenyl Azide

PS Polystyrene

SECTION 1

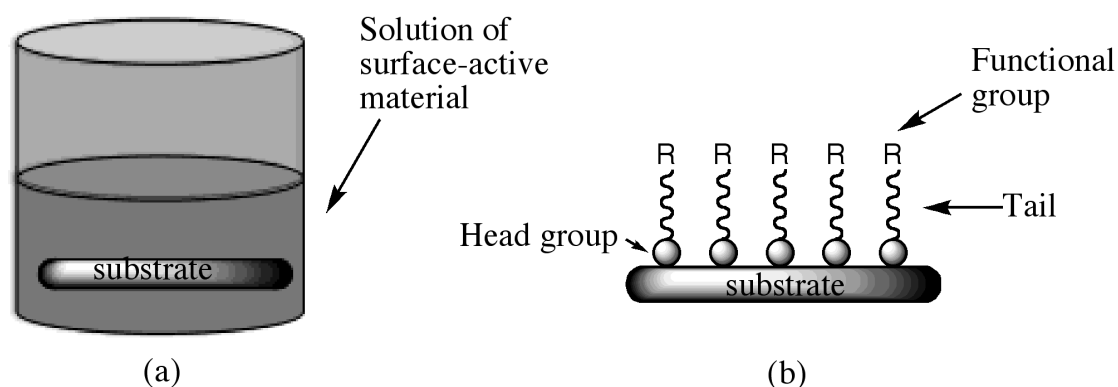
INTRODUCTION

Many traditional and modern applications of material depend not only on the ultimate performance of their bulk properties, but also heavily on the surface microstructure and interface behavior¹. Therefore, the surfaces play an extremely important role in science and technology ranging from sensor technologies and electrochemical devices to micro- and nano-scale systems²⁻⁹. According to the popular scientific database, Elsevier Scopus, the number of papers published in the area of surface modification and applications increased from about 400 per year to 3600 per year in the recent 20 years, reflecting the enormous potential and interest in these topics¹⁰.

Surfaces can be modified by either physical or chemical methods. Physical surface modification methods, in most cases, do not alter the chemical composition and the main purpose is to change the surface state of a material of interest. So physical surface modification methods focus on changes in physical properties like surface roughness, grain sizes and boundaries, and faceting¹¹⁻¹⁷. Chemical surface modification methods can be divided into covalent and non-covalent binding, and physisorption. Normally, covalent linkage to surfaces is preferred over physisorption, which provide a more stable interface.

Self-assembled monolayers (SAMs) has become a highly versatile and general method of surface modification, offering a wide range of opportunities in

microelectronics, optoelectronics, thin-film technology, protective coatings, chemical sensors, biosensors, nanotechnology, bioactive surfaces, cell adhesion, protein adsorption and others¹⁸⁻²¹. SAMs are created by a simple process, shown in Scheme 1.1. The “head groups” of the surface-active molecules are chemisorbed onto a substrate through an organized monomolecular layer with defined orientation. The surface-active molecules spontaneously assemble on the substrate to form stable covalent bonds between its terminal functionality and the substrate. A highly ordered and well-packed functionalized molecular layer thus forms after a period of minutes to hours depending on the reactivity and concentration of the molecule^{8,22,23}. There are two factors that make SAMs superior: (1) a SAM on a planar substrate can be readily prepared in a conventional chemical laboratory by dipping the substrate in a dilute solution of an organic molecule for a specific period of time followed by washing with the same solvent and drying under nitrogen flow; (2) the formation of a SAM needs only a very small amount (approximately 2×10^{-7} g/cm²) of the surface active molecule²⁴. Thus it is economically viable to use even expensive compounds for the development of SAMs.

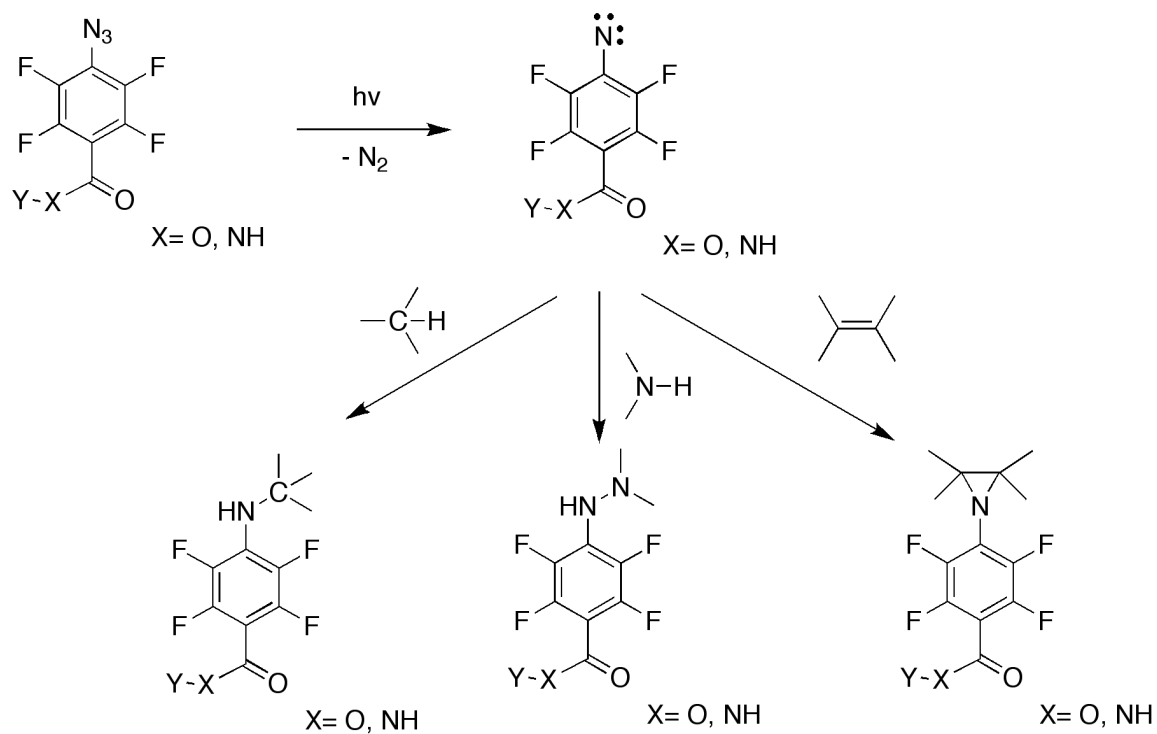


Scheme 1.1 (a) Formation of SAMs by simply immersing a substrate into a solution of the surface-active molecule. (b) Cartoon representation of a SAM on the substrate.

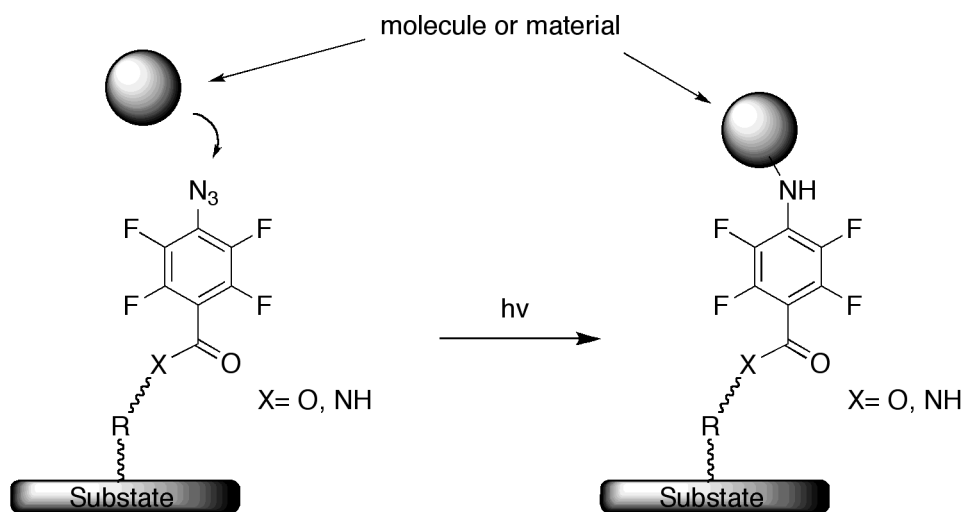
SAMs can be formed on different surfaces depending on the functional groups of the molecule and properties of the surfaces, for example thiols on gold⁸, and silanes on silicon²⁵, which represent the most popular combinations of self-assembling molecules and substrates. One important advantage of silane monolayers assembled on silicon oxide is that they show substantially higher physical and chemical stability in contrast to thiol monolayers on gold. In addition, a broader range of functional silanes can be acquired either from commercial sources or by synthesis, and therefore, additional chemical reactions can be applied to the silane terminal monolayers^{26,27}.

Our laboratory developed a new surface functionalization technique, based on SAM where the R group (Scheme 1.1) is PFPA²⁸. The fluorinated phenylazide has the ability of forming stable covalent linkage under photo or thermal activation. The CH

or NH insertion and C=C addition reactions of the singlet perfluorophenyl nitrene intermediate are the key contributions to the covalent bond formation with the target molecules (Scheme 1.2)²⁸. Due to the versatility of the coupling reactions, the PFPAs have the ability to bind a wide range of molecules and materials including polymers²⁹⁻³¹, small molecules³² and carbon materials³³⁻³⁵. The functional group R can be tailored to be either thiol/disulfide, silane, or phosphate through synthesis, which permits the PFPAs assembly on a wide range of substrates like wafers, glass, metal oxides, and metals in either flat (films), or spherical (nanoparticles) configurations. In addition, PFPA derivatives can be readily synthesized from commercially available starting materials and the products are stable when protected from extensive light exposure. Two distinct and synthetically distinguishable reactive centers, the fluorinated phenyl azide and functional group Y (Scheme 1.2), make the *p*-substituted PFPAs attractive heterobifunctional coupling agents.



Scheme 1.2 CH, NH insertion, and C=C addition reactions of PFPA.



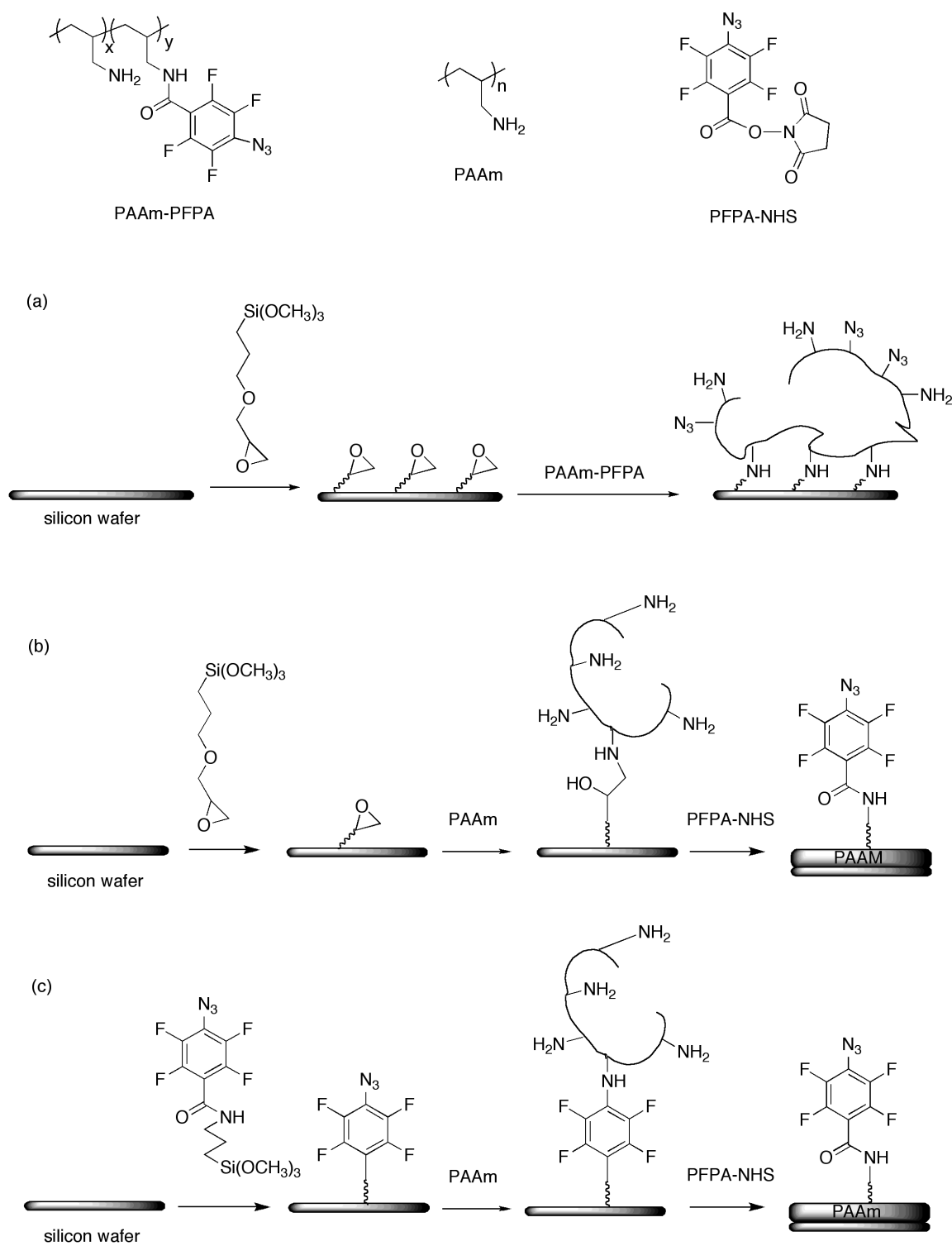
Scheme 1.3 Photo-immobilization of molecules or materials on PFPA surface.

Our research group has demonstrated that PFPA-modified surface can be used to immobilize polymers²⁹⁻³¹, biomolecules³⁶⁻³⁸, and carbon materials like graphene³³⁻³⁵. The immobilization involves a simple process of coating the molecular or material followed by UV irradiation. (Scheme 1.3) However, we found that it is difficult to immobilize nanoparticles on the PFPA surface, and small molecules are attached with a low conjugation efficiency.

The present thesis focuses on developing the second-generation PFPA surface that is based on a polymer matrix. The many repeat units on the polymer will attach more PFPA, thus increasing the density of PFPA on the surface as compared to SAM-based PFPA surface. Moreover, the soft polymer acts as a cushion, allowing for a closer and more conformal contact of the target molecules with the surface. This is of high importance in immobilizing “rigid” materials such as nanoparticles that require the materials to be in close proximity with the PFPA groups on the surface to ensure the photocoupling reaction³⁹.

Three different approaches can be envisioned for the fabrication of polymer-based PFPA surface (Scheme 1.4). In all cases, PAAm was used because it possesses amino groups that can be readily conjugated with, for example, *N*-hydroxysuccinimide (NHS)-functionalized PFPA. In the first approach, PAAm-PFPA is synthesized by reacting PFPA-NHS with PAAm. Epoxy-functionalized surfaces are then treated with PAAm-PFPA. The ratio of the PAAm and PFPA can be controlled to obtain desired density of PFPA. This surface has been successfully used to immobilize nanoparticles and small carbohydrate molecules³².

The current thesis focuses on developing the second and third approaches, shown in Scheme 1.4. These two approaches build PAAm-PFPA directly on the surface by treating PAAm surface with PFPA-NHS. The PAAm surface can be fabricated by treating epoxy-surface with PAAm (Scheme 1.4b) or by immobilizing PAAm on PFPA-surface (Scheme 1.4c). The PAAm-PFPA subsequently surfaces were generated and used to immobilize polymers, nanoparticles, graphene and small carbohydrate molecules. The immobilization efficiencies were compared with those on the PFPA-silane surface. The generated surfaces were characterized with ellipsometry, contact angle goniometry, optical microscopy, and AFM. The bioactivity of the immobilized carbohydrates were evaluated for their binding affinity towards lectins.



Scheme 1.4 Three different approaches for making PAAm-PFPA surfaces.

SECTION 2

EXPERIMENTAL

2.1 Materials

Water used in the experiments was from a Millipore Milli-Q system with at least 17.7 Ω resistivity. Methyl pentafluorobenzoate, *N*-hydroxysuccinimide (NHS), 1-ethyl-3-(3-dimethylaminopropyl)carbodiimide (EDAC) hydrochloride, D-(+)-mannose (Man), 3-aminopropyltrimethoxysilane (APTMS), 3-glycidyloxypropyltrimethoxysilane (GOPTS) were purchased from TCI America. Sodium azide, diethyl ester, silica gel, sodium sulfate (anhydrous), pyridine, *N*-2-hydroxyethylpiperazine-*N'*-2-ethanesulfonic acid (HEPES), tetraethyl orthosilicate (TEOS), poly(2-ethyl-2-oxazoline) (PEOX) (MW 200,000), polystyrene (PS) (MW 280,000) were purchased from Sigma-Aldrich. Concentrated H₂SO₄, H₂O₂ (30%), acetone, methanol, methylene chloride, chloroform, hexane, toluene, hydrochloric acid (HCl), dimethylformamide (DMF), sodium hydroxide (NaOH), sodium chloride (NaCl), calcium chloride (CaCl₂), manganese chloride (MnCl₂), ethanol, 1,2-dichlorobenzene (DCB), ammonium hydroxide (NH₄OH) were purchased from Fisher Scientific. Polyallylamine (PAAm) hydrochloride (MW 120,000) and 4-nitrobenzaldehyde were purchased from Alfa Aesar. 2-*O*- α -D-Mannopyranosyl-D-mannopyranose (Man2) was purchased from Vector Labs Inc. (Covington, Louisiana). Fluorescein concanavalin A (FITC-Con A) was purchased from Vector Lab. Inc. Absolute ethanol (200-proof) was purchased from PHARMCO-AAPER.

Silicon wafers with a 35 Å native oxide layer was purchased from WaferNet, Inc. (San Jose, CA). The long-pass optical filter (280-nm) was purchased from Schott Glass Technologies, Inc. (Fullerton, CA).

2.2 Instrumentation

All irradiation experiments were carried out using a 450 W medium-pressure Hg lamp. AFM images were collected using a Nanoscope MultiMode atomic force microscope (Veeco Metrology) and processed using the software provided by the manufacturer. Dynamic light scattering (DLS) experiments were carried out on a Horiba LB-550 Nano-Analyzer.

Film thickness measurements were performed on a Gaertner Model L116A ellipsometer (Gaertner Scientific Co.) with He/Ne laser (632.8 nm, 2W, Melles Griot) at an incident angle of 70° in the manual mode. The real and imaginary parts of the refractive index of the silicon wafer used in the experiments were 3.870 (N_s) and -0.018 (K_s), respectively. Contact angles were measured on a goniometer (model 250, Ramé-Hart Instrument Co., Netcong, NJ).

Microarray images were recorded on a GenePix4100A microarray scanner with 532 nm laser. UV-vis spectra were recorded on Perkin-Elmer Lambda 45 UV-vis spectrometer.

2.3 Synthesis of PFPA-NHS

The photoactive reagent of PFPA-NHS was synthesized following a previously reported procedure⁴⁰. Briefly, sodium azide and methyl pentafluorobenzoate, were mixed and refluxed for 8 h in a mixed solvent of acetone and water. The crude product was extracted with diethyl ester and dried in vacuum. The residue was re-dissolved in CH₃OH containing 2% NaOH and was stirred overnight. After acidification of the solution to pH<1 with 2M HCl, the solution was extracted with CHCl₃ and dried in vacuum to give 4-azidotetrafluorobenzoic acid. The acid was then react with EDAC and NHS in distilled CH₂Cl₂ under stirring overnight. The resulting mixture was extracted with water and saturated NaCl, and then purified by silica gel chromatography.

2.4 Synthesis of PFPA-silane

PFPA-silane was synthesized according to previously reported procedure⁴¹. PFPA-NHS and 3-aminopropyltrimethoxysilane were mixed in distilled CH₂Cl₂ under stirring overnight. The crude product was purified by silica gel column chromatography to afford PFPA-silane

2.5 Preparation of PAAm-PFPA surface via PFPA

Silicon wafers were cleaned in the piranha solution (3:7 v/v H₂O₂/H₂SO₄) at 80-90 °C for 1 h, washed in boiling water three times for 30 min. each, and dried with nitrogen. The wafers were then treated with a solution of PFPA-silane in toluene (12.6 mM) at room temperature for 4 h, washed with toluene three times for 30 min each, and dried with nitrogen. After curing for at least 24 h, the PFPA-functionalized wafers were soaked in a solution of PAAm•HCl in water (40 mg/mL) overnight. The wafer was removed from the solution, and the excess solution was drained and the sample was allowed to air-dry. The wafer was then covered with a 280-nm long-path optical filter and was irradiated for 9 min with a 450-W medium pressure Hg lamp. The resulting sample was sonicated in 0.1 M HCl three times for 10 min. each followed by in water for 30 min to remove unattached PAAm. The PAAm-modified wafer was then soaked in an aqueous solution of NaOH (pH 12) for about 2 min, washed quickly with absolute ethanol several times and dried with nitrogen.

Finally, the wafer was immersed in a freshly prepared PFPA-NHS solution in DMF (2 mg/mL) at room temperature for 6 h, washed with DMF and ethanol for 30 min each to give the PAAm-PFPA surface.

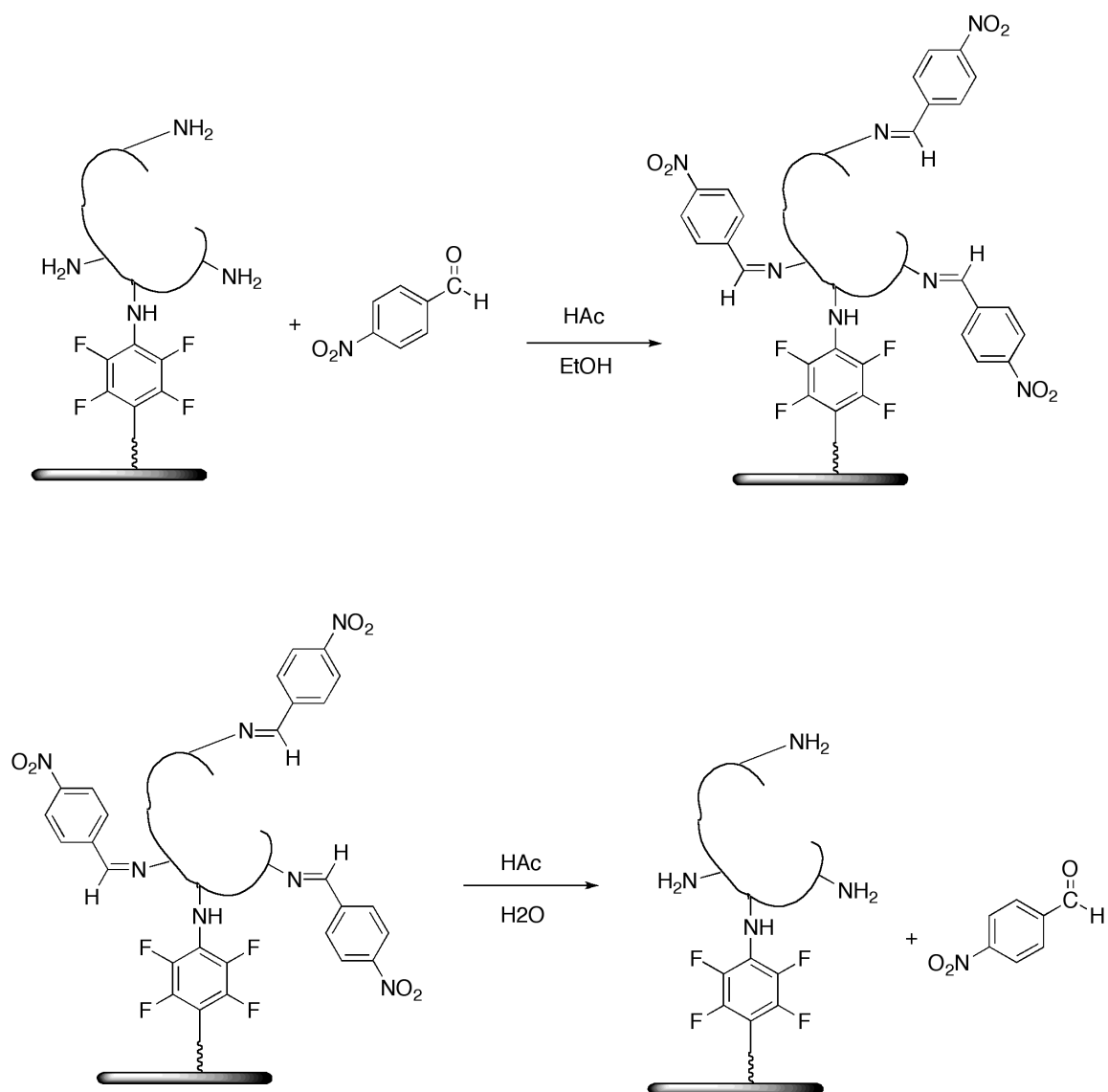
2.6 Preparation of PAAm-PFPA surface on epoxy-functionalized wafer

Piranha-cleaned silicon wafer were treated with a solution of GOTMS in toluene (12.6 mM) at room temperature for 4 h, washed with toluene three times for 30 min each, and dried with nitrogen.

After curing for at least 24 h, the epoxy-functionalized wafers were then soaked in a solution of PAAm•HCl in water/pyridine, and heated at 50 °C for 5 h in the oven. The modified wafers were then washed in HCl for 30 min followed by distilled water for 30 min to remove un-attached polymer. The PAAm-modified wafers were soaked in NaOH (pH 12) for about 2 min, washed quickly with absolute ethanol several times, and dried with nitrogen. Finally, the wafers were immersed in a freshly made PFPA-NHS solution in DMF (2 mg/mL) at room temperature for 6 h, washed with DMF and ethanol for 30 min each to give the PAAm-PFPA surface.

2.7 Determination of amine density of PFPA-PAAm surface by UV-vis spectrometry

The free amino groups on the surface were measured by reacting the PAAm-functionalized wafers with 4-nitrobenzaldehyde to form imine. The imine was then hydrolyzed in a known volume of water to release 4-nitrobenzaldehyde and the absorbance of the released 4-nitrobenzaldehyde was recorded by UV-vis spectroscopy (Scheme 2.1). By measuring the amount of 4-nitrobenzaldehyde released, the density of the surface amine can be calculated. Both reactions happen under acidic conditions⁴².



Scheme 2.1 Determination of surface amine density by forming imine and releasing 4-nitrobenzaldehyde.

In the experiment, a PAAm-functionalized wafer (1 inch²) was immersed in anhydrous ethanol (25 mL) containing 4-nitrobenzaldehyde (10 mg) and acetic acid (20 μ L), and the wafer was then incubated in an oven at 50 $^{\circ}$ C for 3 h. The wafer

was washed with absolute ethanol by sonication three times for 1 min each, and dried with nitrogen. The resulting imine substrate was hydrolyzed in water (5 mL) containing acetic acid (10 μ L) at room temperature overnight, after which, the wafer was rinsed with the same amount of solvent (5 mL water containing 10 μ L acetic acid). The two wash solutions were combined and the absorbance at 267 nm was measured using a UV-vis spectrometer. A calibration curve was generated by preparing various concentrations of 4-nitrobenzaldehyde (0-100 μ M) in the same solvent and absorbance at 267 nm measured and plotted against 4-nitrobenzaldehyde concentration.

2.8 Preparation of glyconanoparticles

Silica nanoparticles (SNPs) were synthesized using the Stober protocol^{43,44}. Briefly, TEOS (2.8 mL) was added to 200 proof absolute ethanol (34 mL) followed by 25% NH_4OH (2 mL). The mixture was capped and allowed to react at room temperature for 24 h with vigorous stirring to yield a colloidal solution. This recipe resulted in particles that were \sim 40 nm in diameter, as measured by DLS.

The freshly made PFPA-silane (80 mg) was added directly to the Stober solution and the mixture was stirred at room temperature overnight followed by at 78 $^{\circ}\text{C}$ under reflux for 1 h. The PFPA-functionalized SNPs were isolated by centrifugation (12,000 rpm, 45 min) and then redispersion in the fresh solvent by sonication. This

centrifugation/redispersion procedure was repeated three times with absolute ethanol and twice with acetone.

The solution of PFPA-functionalized SNPs in acetone (5 mL) was placed in a flat-bottom dish, and an aqueous solution of carbohydrate (10 mg/mL, 1 mL) was added. The mixture was covered with a 280-nm long-path optical filter and was irradiated with a 450-W medium pressure Hg lamp for 10 min under vigorous stirring. Excess carbohydrates were removed by centrifugation (12,000 rpm, 45 min) and the particles were redispersed in water by sonication three times. The sizes of the resulting glyconanoparticles were measured by DLS.

2.9 Immobilization of polymers

A solution of PS or PEOX in chloroform (10 mg/mL) was spin-coated (2,000 rpm, 60 s) on the PAAm-PFPA surface or wafers treated with PFPA-silane. The sample was covered with a 280-nm long-path optical filter and was irradiated for 9 min with a 450-W medium pressure Hg lamp. The wafers were then washed 3 times for 10 min each by sonication. The thickness of the immobilized polymers was measured by an ellipsometer.

2.10 Immobilization of nanoparticles

An aqueous solution of glyconanoparticles (0.5 μL) was dropped onto the PAAm-PFPA or PFPA-silane surface from a pipettor tip. After drying the samples in vacuum, the wafers were covered with a 280-nm long-path optical filter and were irradiated for 9 min with a 450-W medium pressure Hg lamp. The excess nanoparticles were removed by sonicating the samples in water and ethanol for 5 min each and dried with nitrogen. The resulting samples were imaged by AFM in the contact mode.

2.11 Immobilization of graphene

Graphene flakes were prepared by sonicating graphite particles (50 mg) in DCB (20 mL) for 1 h using a sonication probe. The mixture was settled for 1 week, and the supernatant was centrifuged at 4,600 rpm for 30 min. The upper solution was dropped on the PAAm-PFPA and PFPA-silane surface and dried in air. The wafers were then covered with a photomask and were irradiated for 9 min with a 450-W medium pressure Hg lamp. The unattached graphene was removed by sonication in DCB for 5 min. The samples were imaged using an optical microscope.

2.12 Immobilization of carbohydrate

An aqueous solution of Man2 (10 mg/mL) was printed onto the PAAm-PFPA and PFPA-silane surface using a robotic printer (BioOdyssey Calligrapher miniarrayer;

Bio-Rad Laboratories, Inc.). After drying in vacuum, the wafer was spin-coated with a solution of PEOX in chloroform (10 mg/mL) at 2,000 rpm for 1 min. After irradiated with a 450-W medium pressure Hg lamp in the presence of a 280-nm long-path optical filter for 9 min, the wafer was washed in chloroform and water by sonication for 5 min each. Finally, the wafer was soaked in a solution of FITC-Con A (0.5 mg/mL) in HEPES buffer (10 mM) containing MnCl_2 (1 mM), CaCl_2 (1 mM) and NaCl (100 mM) overnight, rinsed with the same HEPES buffer and dried with nitrogen. GenePix 4100A Microarray Scanner was used to obtain the fluorescence images of the samples.

SECTION 3

RESULTS AND DISCUSSION

The key objective of this thesis is to prepare a PAAm-based PFPA surface that can be used to attach a variety of materials especially nanoparticles, graphene and small molecules. To achieve this, two procedures were developed for the preparation of PAAm-PFPA surface (Scheme 1.4b, c). In the first approach, PAAm was first immobilized on the PFPA surface, and PFPA was subsequently introduced by reacting PFPA-NHS with the surface PAAm layer. In the second approach, PAAm was immobilized on epoxy-functionalized surface before treating with PFPA-NHS.

3.1 Preparation of PAAm-PFPA surface via PFPA

The PFPA-surface was prepared following a previously-established procedure⁴⁵ by soaking piranha-cleaned silicon wafers in a freshly made PFPA-silane solution in toluene (12.6 mM) for 4 hours. To ensure a monolayer formation, the thickness of every sample was monitored by ellipsometry. A thickness of around 10 Å (Figure 3.1) is a good indication that a monolayer of PFPA-silane had formed on the piranha-cleaned wafer. We found that it was challenging to immobilize PAAm on PFPA-surfaces because the surface was fairly hydrophobic (static water contact angle $\sim 80^\circ$). Because PAAm is only soluble in water, a thin film cannot be obtained by spin coating due to the high vapor pressure of water. Dropping the aqueous solution of PAAm•HCl (40 mg/mL) on the PFPA-functionalized wafers and drying in

the hood overnight gave a hydrogel film. However, the film was thick and uneven. Furthermore, after UV irradiation, only a very thin film remained after solvent extraction, probably because the thick layer prevented the UV light from passing through. Finally, the PFPA-functionalized wafers were soaked in the aqueous solution of PAAm•HCl (40 mg/mL) for 12 hours. The surface changed from hydrophobic to hydrophilic, indicating that a polymer layer was adsorbed on the surface. The excess PAAm solution was drained from the sample and was allowed to air-dry to give a thin film. After UV irradiation and solvent extraction to remove unbound PAAm, a PAAm layer of about 30~40 Å in thickness was obtained (Figure 3.1).

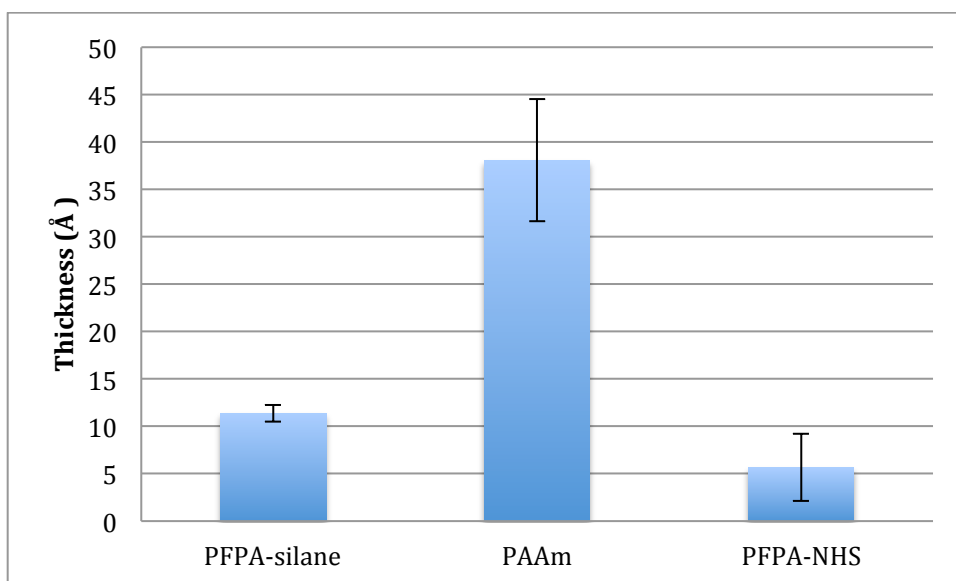


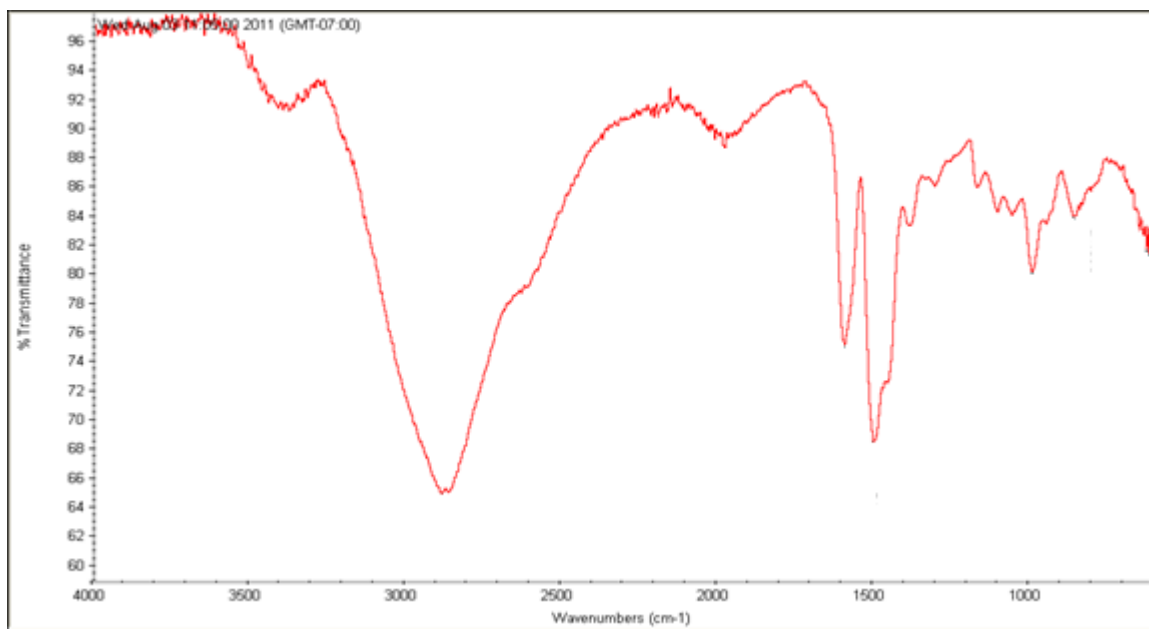
Figure 3.1 The thickness of different surface layers. Each data point was an average of 5 measurements.

To prepare PAAm-PFPA surface, the polymer-coated wafers were first treated with NaOH to convert PAAm•HCl to the free amine, which would react with the PFPA-NHS to provide the final surface. The samples were dipped briefly in NaOH for 2 min and rinsed immediately with absolute ethanol. The samples were then soaked in a solution of PFPA-NHS in DMF (2 mg/mL) to give the PAAm-PFPA surface with a layer thickness of about 5-15 Å (Figure 3.1).

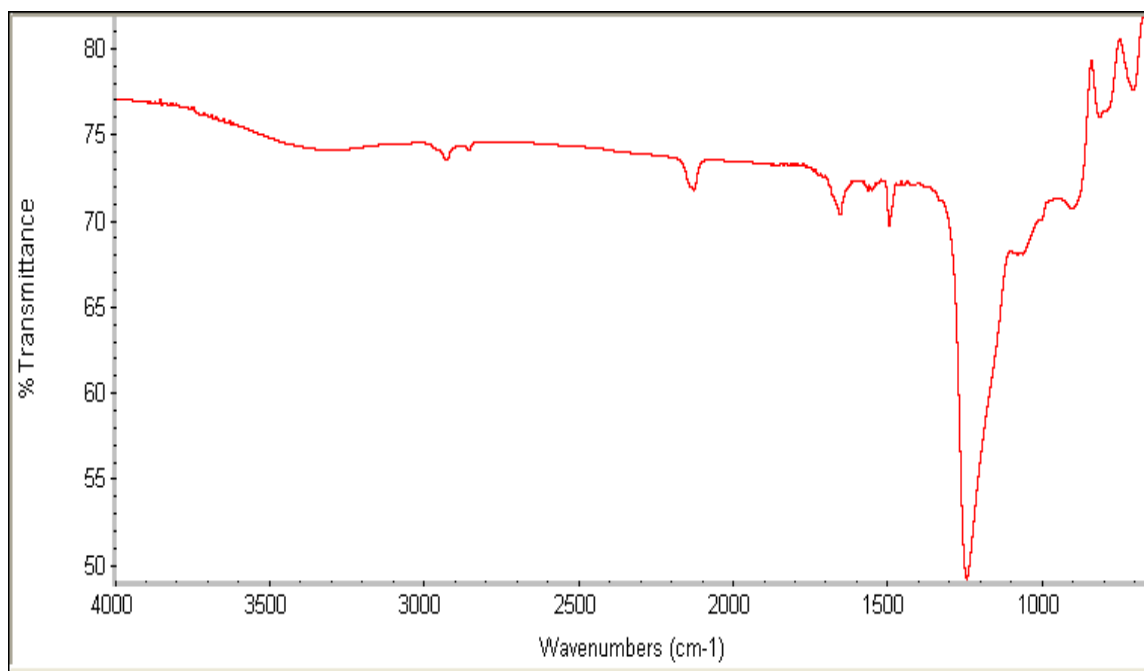
To further confirm that the PAAm-PFPA surfaces were successfully made, the surfaces were characterized by ATR-IR. In the IR spectrum of bulk PAAm•HCl (Figure 3.2a), the broad peak around 3376 cm⁻¹ came from the stretching of N-H, while the strong peak around 1600 cm⁻¹ and 1500 cm⁻¹ came from the bending absorption of N-H. Figure 3.2b is the ATR-IR spectrum of the surface functionalized with PFPA-silane. The peaks around 2930 cm⁻¹ and 2850 cm⁻¹ were stretching bands of methylene hydrogens where the 2930 cm⁻¹ absorption was from the asymmetric mode which generates a larger dipole moment and is of greater intensity than the peak at 2850 cm⁻¹ that was from the symmetric mode. The peak around 2120 cm⁻¹ was from azido group⁴⁶, and the peaks around 1650 cm⁻¹ and 1500 cm⁻¹ were from the secondary amide of the PFPA-silane. Figure 3.2c shows the spectrum of the PAAm layer that was immobilized on PFPA. Compared to the Figure 3.2b, the intensity of the peaks from the CH stretching bands of methylene increased, which resulted from the increasing concentration of the methylene group of in PAAm. The peak of the azido group disappeared because they had reacted to bind PAAm on the surface. Since the top layer of the surface was PAAm•HCl, the peaks of primary

amine salts at 1610-1500 cm^{-1} dominated the peak from the amide. Because there were limited amount of materials on the surface, only strong peaks showed up, and some weak peaks may not be detected such as the stretch of primary amine salts, which should be observed at 2890 cm^{-1} . Figure 3.2d is the ATR-IR spectrum of the PAAm-PFPA surface after the PAAm surface was treated with PFPA-NHS. The azide peak was not detected in the spectrum. From the thickness data, the PFPA-NHS was on the surface (Figure 3.1). The absence of the azide peak might be due to the thick PAAm underlayer that diluted the concentration of the surface PFPA. In fact, the spectrum is very similar to that of PAAm surface (Figure 3.2).

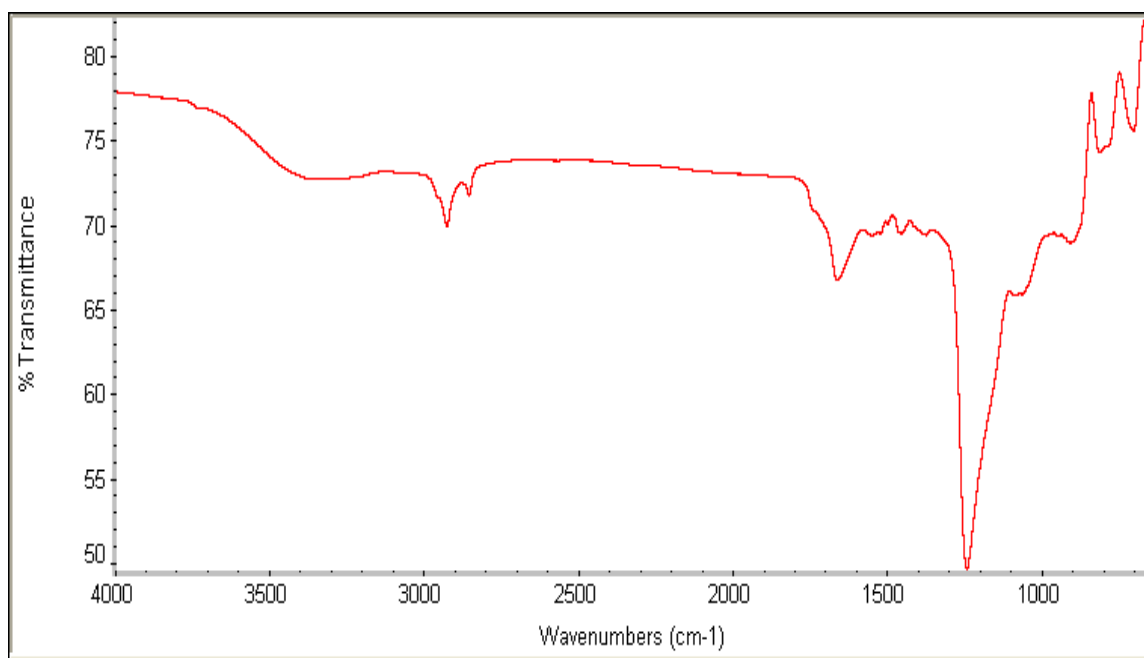
a)



b)



c)



d)

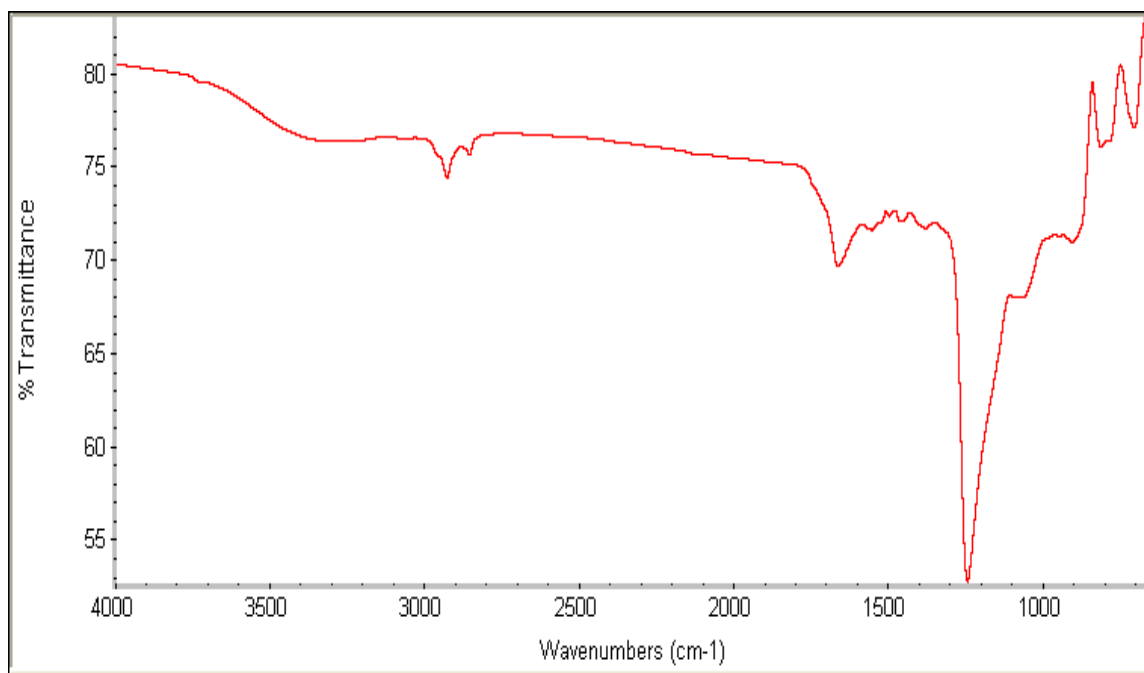


Figure 3.2 (a) IR spectrum of bulk PAAm•HCl, ATR-IR spectra of (b) PFPA, (c) PAAm surface, and (d) PAAm-PFPA surfaces.

3.2 Amine density determination of the PAAm surface

To further confirm that PAAm was successfully immobilized on PFPA-functionalized surface, the density of amino groups was determined. This was carried out by reacting the PAAm-functionalized wafers with 4-nitrobenzaldehyde to form imine under acidic conditions in ethanol⁴⁷. After the wafers were cleaned with fresh solvent to remove excess reagents, the surface imines were hydrolyzed also under acidic conditions (Scheme 2.1). Because aldehyde is stoichiometrically equivalent to

that of amino groups on the surface, by measuring the amount of 4-nitrobenzaldehyde released, the density of free amino groups can be calculated. The amount of 4-nitrobenzaldehyde was determined spectroscopically. The maximum absorption of the aqueous solution of 4-nitrobenzaldehyde is at 267 nm measured by UV-Vis spectroscopy. A calibration curve was obtained by measuring the absorption at 267 nm against the concentration of 4-nitrobenzaldehyde (Figure 3.3).

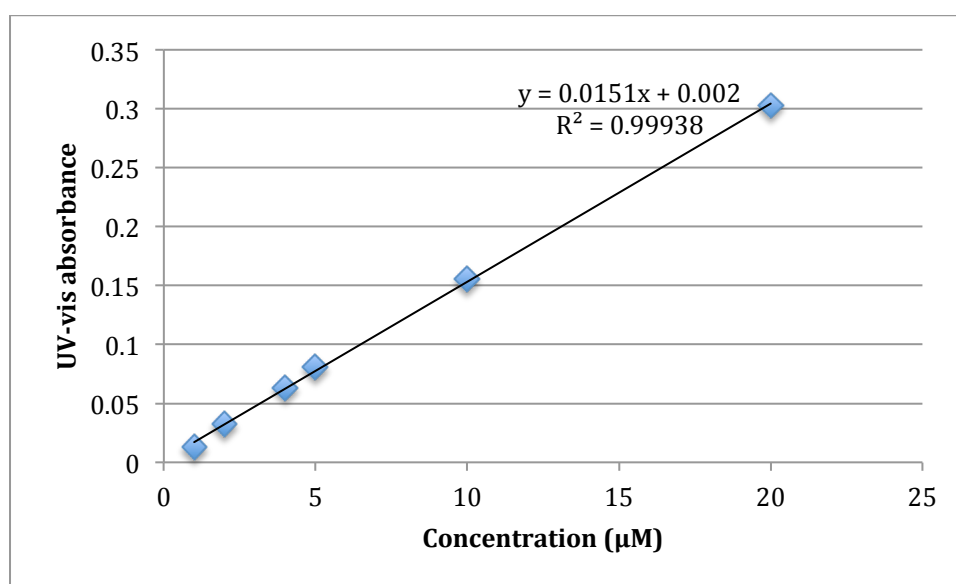


Figure 3.3 Standard calibration curve of 4-nitrobenzaldehyde by measuring the maximal UV-Vis absorbance of the solution at 267 nm against its concentration.

According to Beer's Law:

$$A = \epsilon bc$$

from Figure 1, ϵ was calculated to be $0.015 \text{ cm}^{-1} \mu\text{M}^{-1}$

Table 3.1 Surface concentration of amino groups on PAAm and PFPA surfaces (2.54×2.54 cm²).

Sample	A	c (M) ¹	Surface concentration (No. of amino groups/nm ²)
PAAm surface	0.0544±0.002	3.60 * 10 ⁻⁶	33.8±0.1
PFPA surface	0.0009±0.0003	6.15 * 10 ⁻⁸	0.6±0.2

¹ $c = A/\epsilon b$ where $\epsilon = 0.015 \text{ cm}^{-1}\mu\text{M}^{-1}$ and $b = 1 \text{ cm}$.

² Surface concentration = $c \cdot N_A / S$, where N_A is Avogadro's number (6.02×10^{23}) and S is the surface area of the sample ($1 \text{ inch}^2 = 6.45 \times 10^{14} \text{ nm}^2$). Each data was the average of 3 measurements.

The amine density of both the PAAm surface and PFPA surface was measured, and results are shown in Table 3.1. Significantly higher amount of amino groups were present on the PAAm surface as compared to the PFPA surface, which demonstrated that PAAm was successfully immobilized on PFPA surface. The density, 33.8 molecules/nm², represents a high amine concentration when comparing the values reported in the literature, which had the density of 37.3 molecules/nm².⁴⁸ This surface was fabricated by using gold films modified with poly (L-lysine) followed by PFPA-NHS.

3.3 Preparation of PAAm-PFPA from epoxy surface

The second approach to prepare PAAm-PFPA surfaces started from the epoxy-functionalized wafers. The epoxy functional groups were generated by treating piranha-cleaned wafers with GOTMS solution in toluene (12.6 mM) for 4 hours. The thickness of the epoxy layer, ~ 9 Å, indicated that a monolayer was likely formed³². However, after treating the epoxy wafers with PAAm and then PFPA-NHS, the thickness did not change significantly (Figure 3.4). The IR spectra of PAAm and PAAm-PFPA surfaces were also identical (Figure 3.5a, b). One possibility was that all amino groups on PAAm reacted with epoxy groups. In this case the polymer would stretch out to allow its side chain (methylamino groups) to react with the surface epoxy groups. This flattened conformation would give very small thickness, which might be difficult to detect by ellipsometry. In addition, because all amino groups on PAAm had the opportunity to react with the epoxy groups, this would consume significantly higher percentage of free amino groups on PAAm leaving very small amount of free amino groups to react with PFPA-NHS. The fact that the thickness was not measurable after reaction with PFPA-NHS also supported the hypothesis that very small amount of PFPA-NHS was attached. This hypothesis has been further validated by the subsequent immobilization studies shown in the sections that follow.

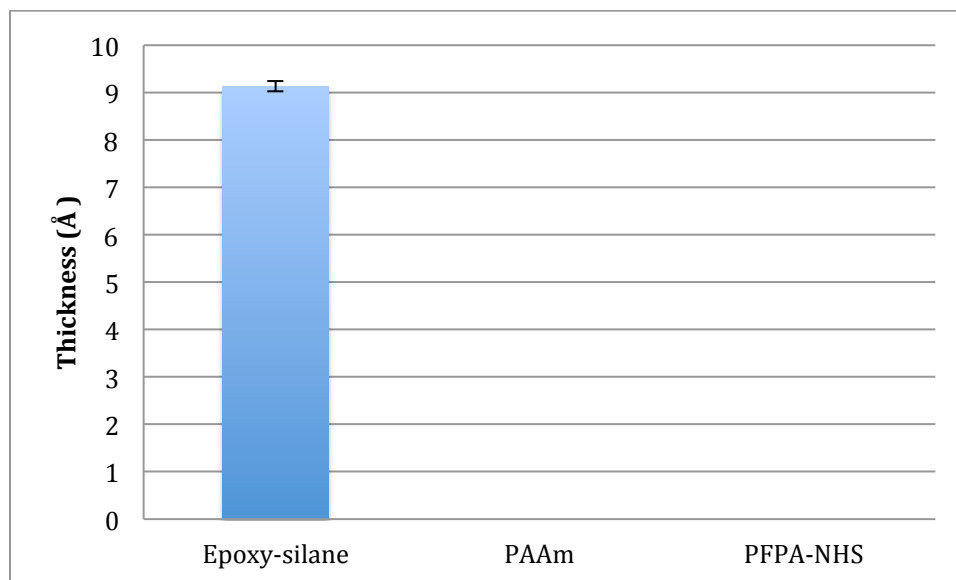
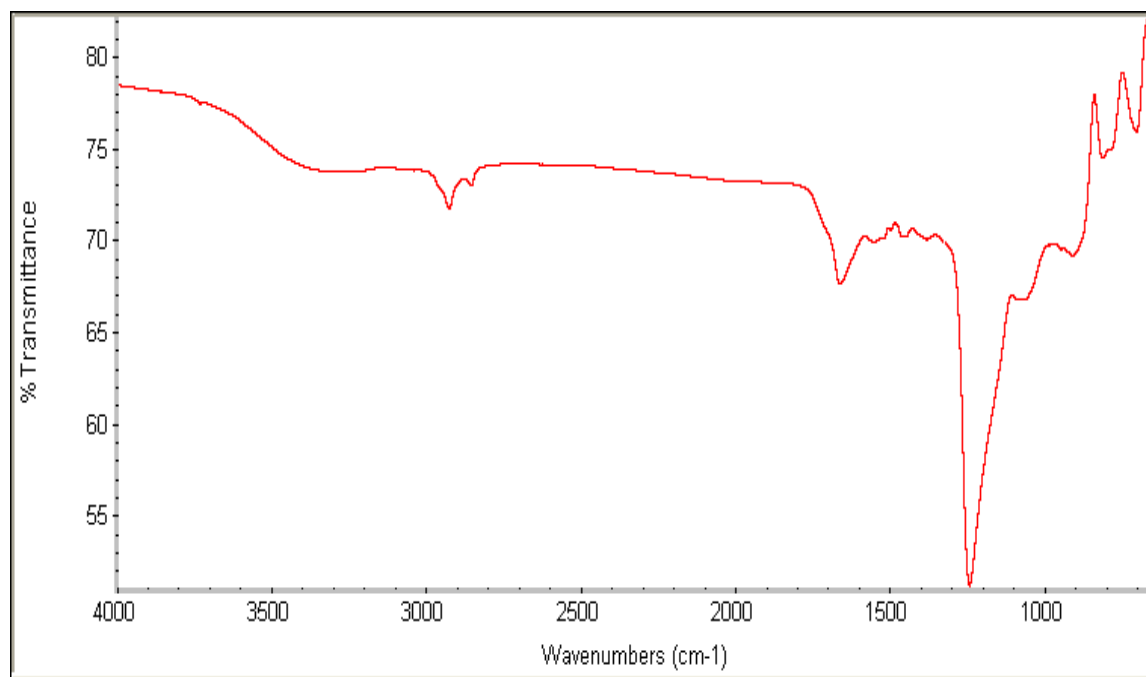


Figure 3.4 The thickness of different layers of epoxy-PAAm-PFPA surface. The thickness of the PAAm layer or PFPA-NHS layer could be detected by ellipsometer. Each data point was an average of 5 measurements

a)



b)

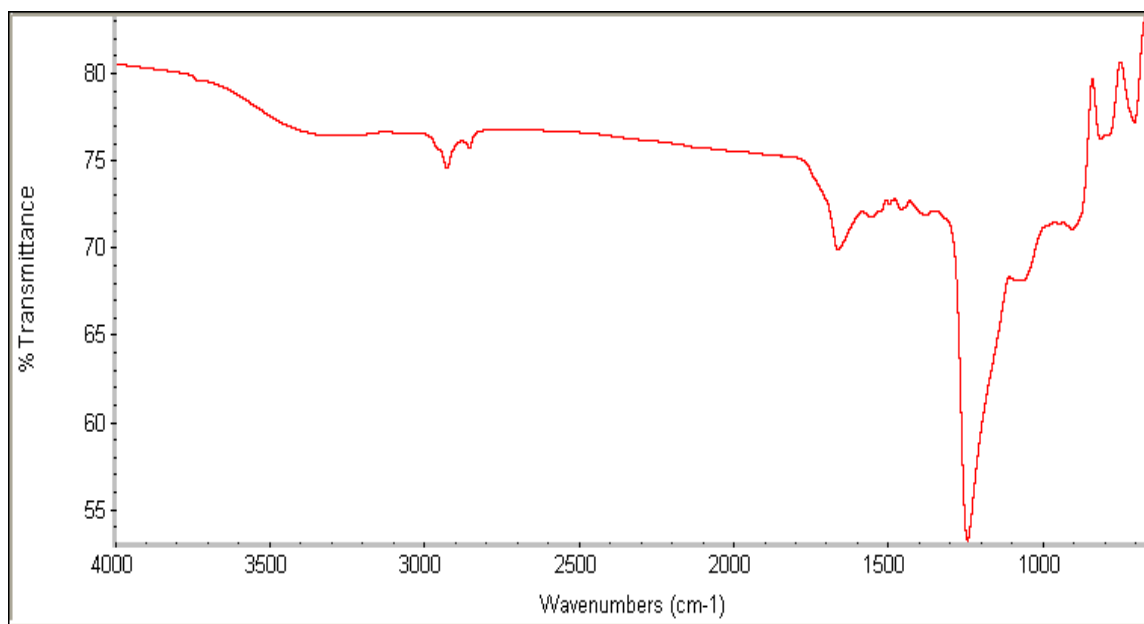


Figure 3.5 ATR-IR spectra of (a) PAAm, and (b) PAAm-PFPA surfaces fabricated on epoxy surface.

3.4 Immobilization of polymers

To determine the effectiveness of the designed surfaces for the immobilization of polymers, a solution of PS in chloroform was spin coated on the PAAm-PFPA surfaces followed by UV irradiation in the presence of a 280 nm long-path optical filter to remove the deep-UV light that can crosslink the polymer. After removing the excess PS by sonicating the sample in chloroform, a thin film of ~ 56 Å in thickness remained on the surface (Figure 3.6). This value is similar to the thickness of PS films immobilized on the surfaces functionalized with PFPA-silane (Figure 3.6). A

control sample was prepared by spin-coating PS on PAAm surface. After UV irradiation and removal of excess PS, the thickness of the PS thin film was not detectable (Figure 3.6). This result demonstrated that PS was immobilized by PFPA rather than physisorption on PAAm. In addition to PS, other polymers like PEOX was also successfully immobilized on the PAAm-PFPA surface (Figure 3.6). The results confirmed that PAAm-PFPA surfaces were successfully prepared and that the resulting surfaces have the ability to immobilize polymers effectively.

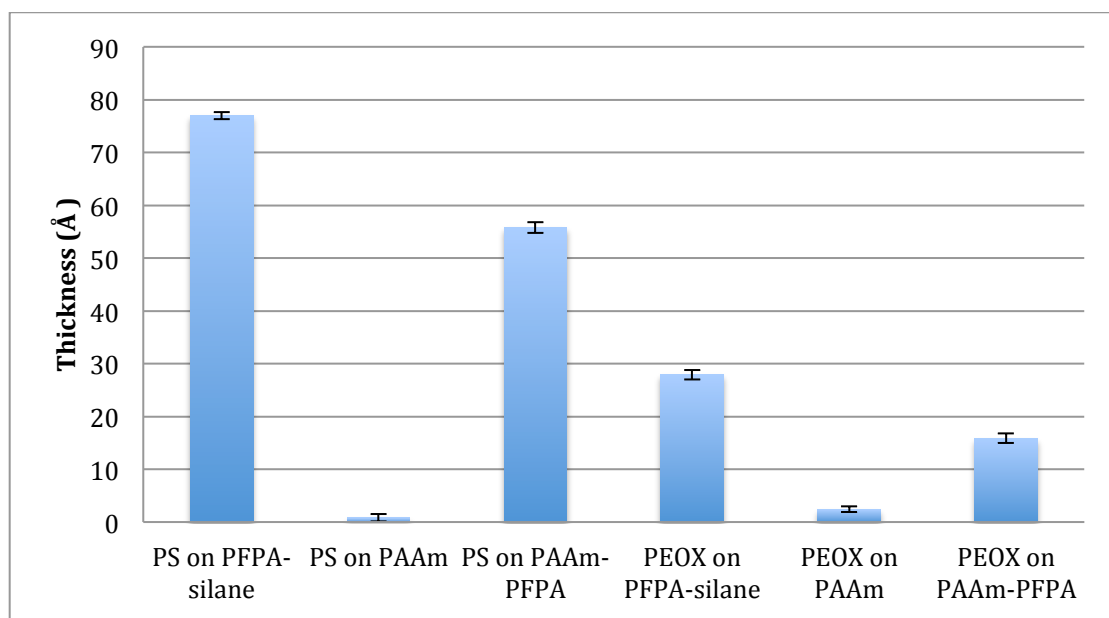


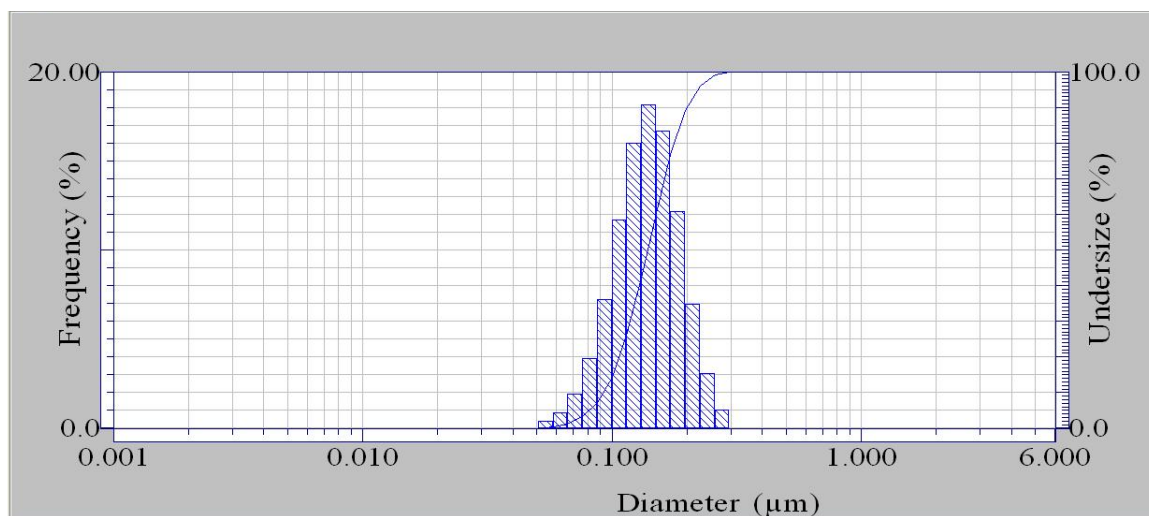
Figure 3.6 The thickness of PS and PEOX immobilized on different surfaces. Each data point was an average of 5 measurements

3.5 Immobilization of nanoparticles

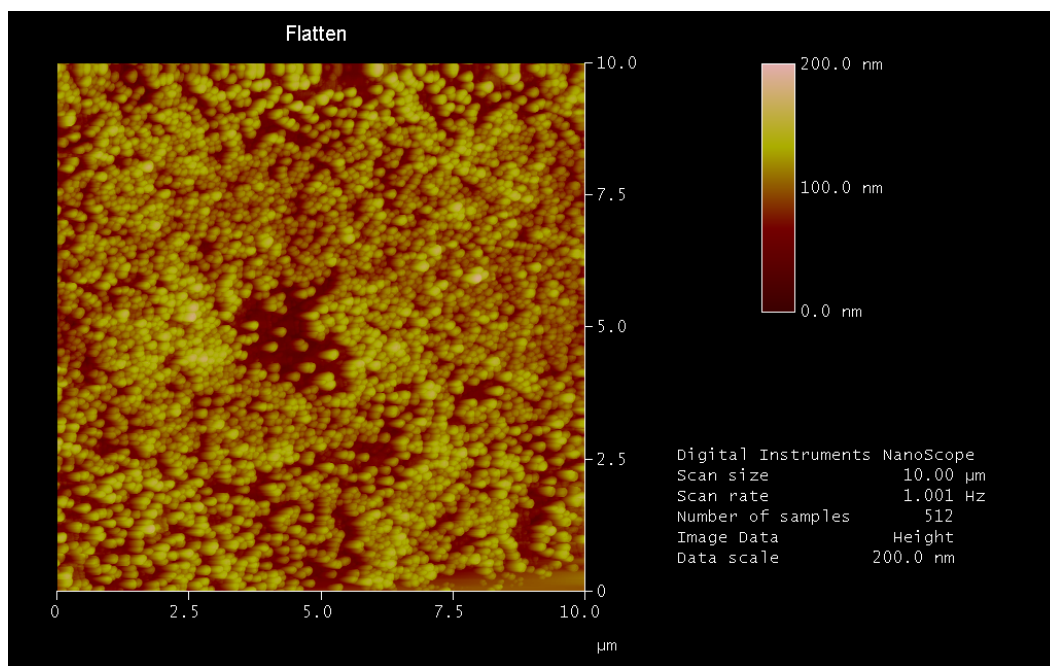
To test the ability of PAAm-PFPA in immobilizing of nanoparticles, silica NPs functionalized with carbohydrates were used. Silica NPs, ~140 nm in diameter measured by DLS (Figure 3.7a), were synthesized using the Stober protocol^{43,44}. They were then functionalized with PFPA-silane on and Man was subsequently conjugated by previously established photocoupling process by irradiating the mixture of PFPA-NPs and Man^{36,37}. The Man-functionalized silica NPs were obtained after dialysis to remove excess reagents. The particles were then dropped on the PAAm-PFPA surface by using a pipet tip, followed by UV irradiation and rinsing with solvent. The particles were immobilized on the surfaces successfully and can be visualized by AFM (Figure 3.7b, c). The size of the immobilized particles observed using AFM were consistent with the diameters of the corresponding nanoparticles measured by DLS. However, when the nanoparticles were coated on PFPA-silane-functionalized wafer, almost no particles remained on the surface after UV irradiation and solvent rinsing (Figure 3.7c). This result is consistent with our hypothesis that the polymer-based PFPA surface is more efficiently in immobilizing solid materials such as nanoparticles. In order for the CH insertion reaction to occur, the particles need to be in close contact with the surface azido group⁷. Because of the spherical geometry of the nanoparticles, their contact area with the PFPA surface was very limited. The polymer-based PFPA surface, PAAm-PFPA, is softer which would enhance the contact between the nanoparticles and the surface. The PAAm-PFPA layer is also rougher, which could further increase the contact areas

with the nanoparticles. In addition to 140 nm particles, glyconanoparticles of smaller particle size (~ 40 nm) (Figure 3.7e) were also synthesized and successfully immobilized on the PAAm-PFAP surface. In this case, significantly lower concentration of the glyconanoparticles (0.6 mg/mL) was used to coat the PAAm-PFPA surface than the larger 140 nm glyconanoparticles (112 mg/mL), yet high density particles could be immobilized. As can be seen from the DLS and AFM images, the smaller nanoparticles were irregular and were not as spherical or uniform as the larger ones. This particle irregularity effectively increases the contact area with the PAAm-PFPA surface and the immobilization was thus enhanced as a result.

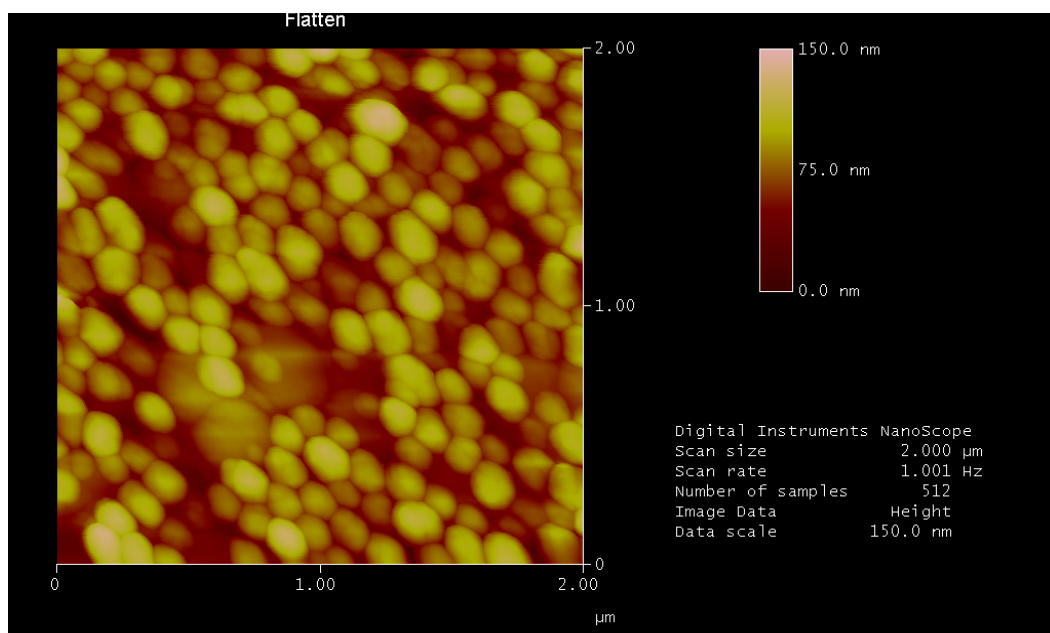
a)



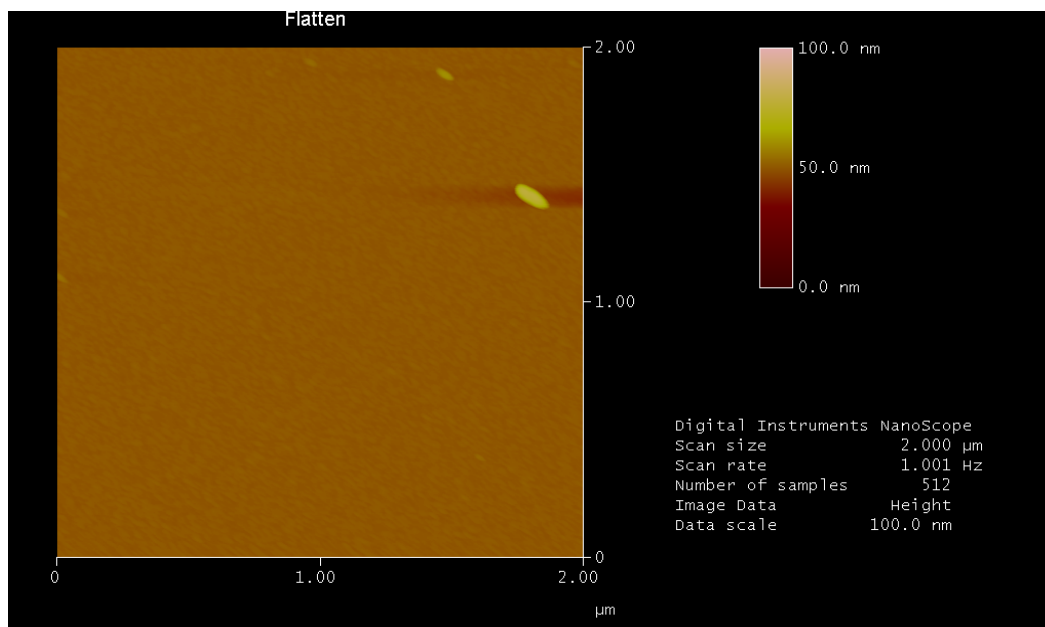
b)



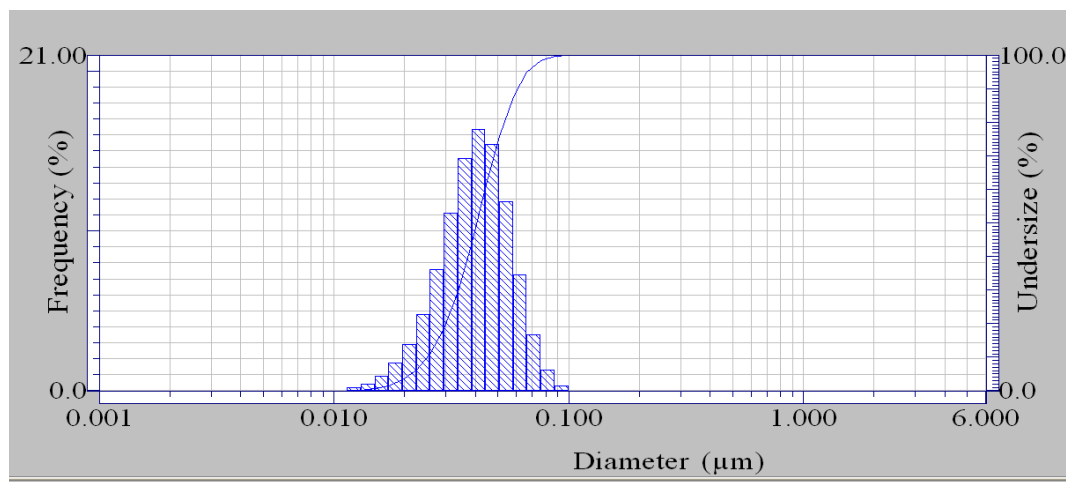
c)



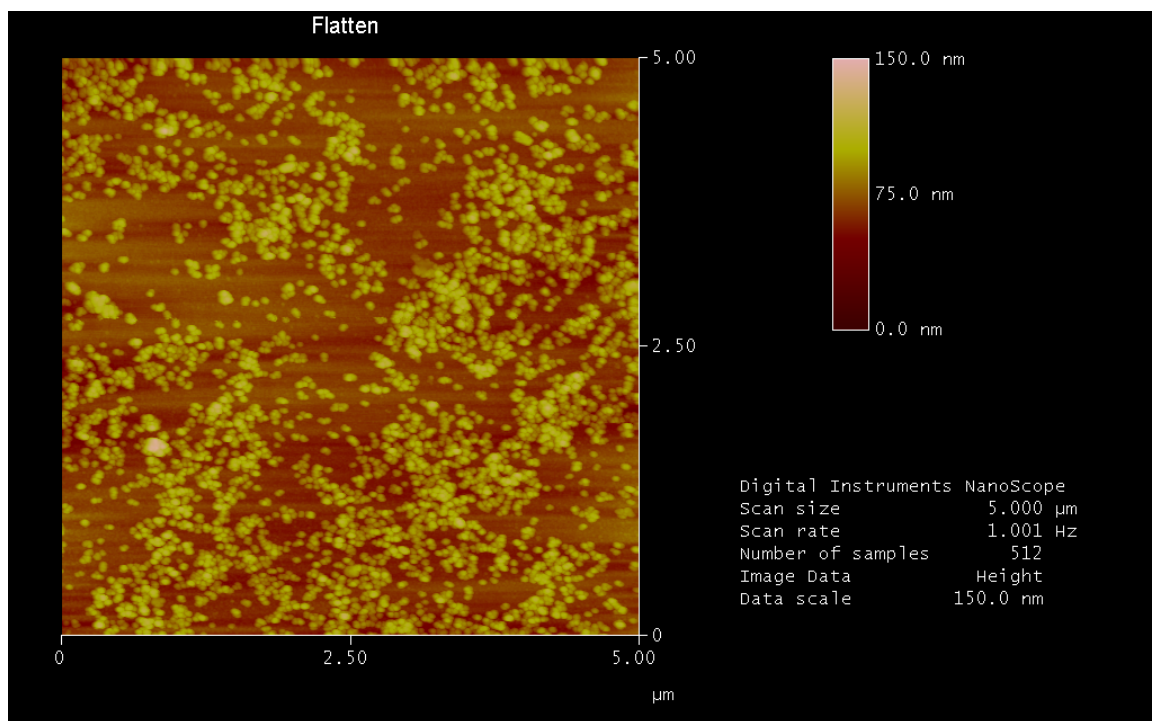
d)



e)



f)



g)

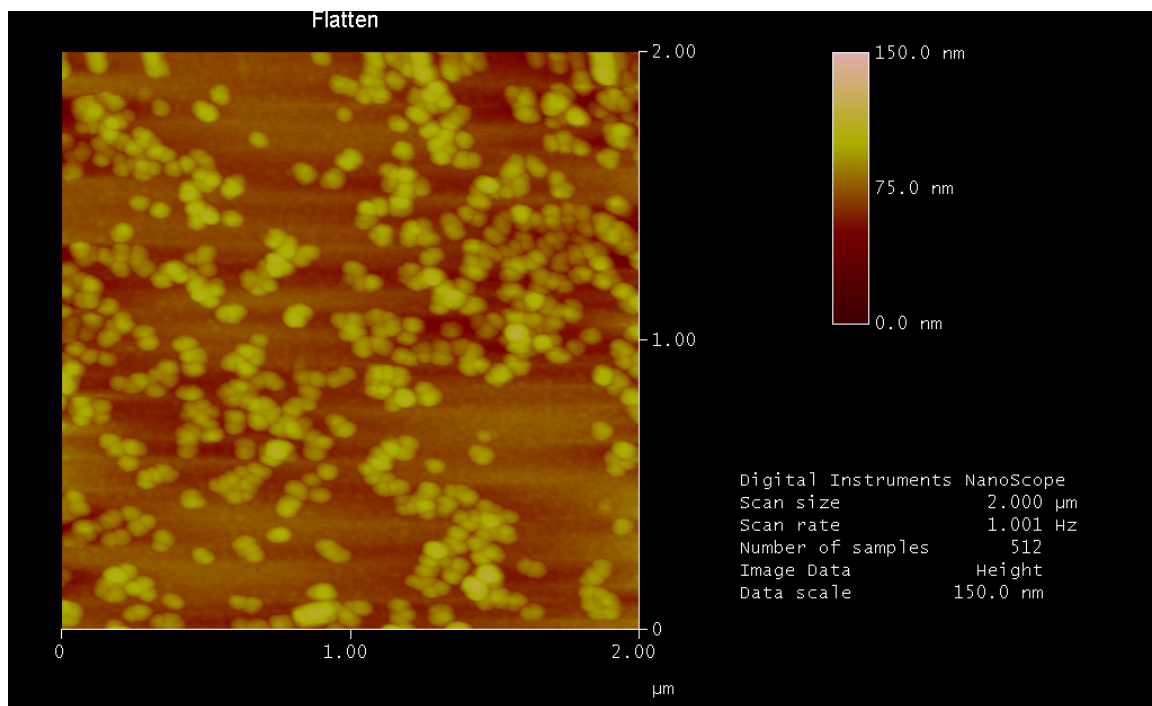


Figure 3.7 (a) DLS of 140 nm glyco-nanoparticles. AFM images of 140 nm glyconanoparticles immobilized on (b, c) PAAm-PFPA and (d) PFPA-silane surface. (e) DLS of 40 nm glyconanoparticles. AFM images of 40 nm glyconanoparticles immobilized on (f, g) PAAm-PFPA surface.

3.6 Immobilization of graphene

Similar to nanoparticles, graphene is also a solid material that is difficult to form conformal contact with the hard silicon wafer surface. The polymer-based surface offers a softer cushion that should provide a better immobilization efficiency for graphene than the PFPA-silane surface. To test this, graphene flakes were prepared by sonicating graphite particles in DCB followed by multiple time of centrifugation to remove larger particles. The upper solution containing graphene flake in DCB was dropped on both PAAm-PFPA and PFPA-silane surfaces. After drying in the hood, the samples were UV irradiated in the presence of a photo mask followed by sonication in DCB to remove excess graphene flakes. The optical images of the resulting surfaces show the successful immobilization of graphene on both surfaces (Figure 3.8b, d). However, on the PAAm-PFPA surface (Figure 3.8b), the patterns were much clearer than on the PFPA-silane surface (Figure 3.8d) revealing a higher density of graphene flakes on the PAAm-PFPA surface. This is consistent with the hypothesis that the PAAm-PFPA surface provides a better and more conformal contact with solid materials such as graphene. A control experiment was carried out

by UV irradiating a graphene covered PAAm-PFPA surface without the photomask. In this case, no patterns were visible and graphene flakes were observed on the entire surface (Figure 3.8c).

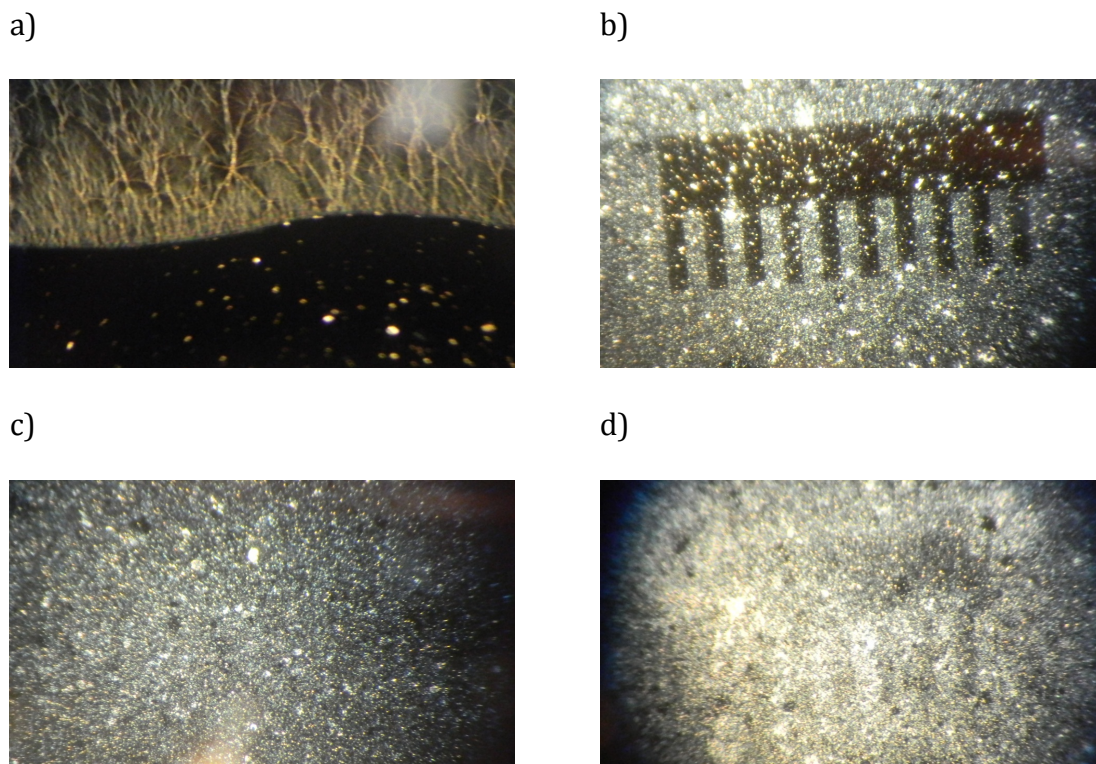


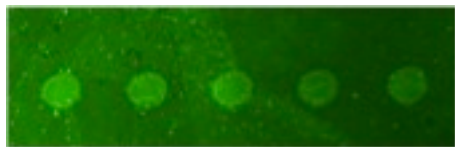
Figure 3.8 Optical images (100 \times) of graphene on PAAm-PFPA surface (a) before UV irradiation, (b) after UV irradiation with a photomask, (c) after UV irradiation without the photomask, and (d) graphene on PFPA-silane surface after UV irradiation with the photomask. The negative imaging mode was used, and the surface covered by graphene was brighter than the surface without graphene.

3.7 Immobilization of carbohydrates

To test the effectiveness of the PAAm-PFPA surface for the immobilization of small molecules, Man2, a disaccharide, was used. Because Man2 exhibits specific affinity to Con A, a plant lectin, a functional binding assay can be performed to test the immobilized Man2.

Man2 was immobilized by printing an aqueous solution of Man2 (10 mg/mL) on the PAAm-PFPA or PFPA-silane surface using a robotic printer. After drying, a solution of PEOX in chloroform (10 mg/mL) was spin-coated on the surface. PEOX was used as the anti-fouling coating to reduce the non-specific adsorption of proteins in the subsequent binding assays⁴⁹. Because Man2 is insoluble in organic solvent, PEOX can be spin-coated from the chloroform solution without disturbing the spotted Man2. The sample was then irradiated with UV light for 9 min to covalently attach both Man2 and PEOX on the surfaces. The unattached PEOX and Man2 were removed by sonicating in chloroform and water. The resulting samples were then incubated in a solution of FITC-Con A in HEPES buffer (10 mM) containing MnCl_2 (1 mM), CaCl_2 (1 mM) and NaCl (100 mM), rinsed with the fresh HEPES buffer and dried. The Man2 spots on the PAAm-PFPA surface were brightly fluorescent (Figure 3.9a) whereas very weak signals were observed on the PFPA-silane surface (Figure 3.9b). The significantly enhanced signals from the PAAm-PFPA surface was a strong evidence that the polymer-based PAAm-PFPA surface was much more efficient in immobilizing small molecules such as Man2.

a)



b)



Figure 3.9 Fluorescence images of immobilized Man2 spots after treating with FITC-Con A. Man 2 was immobilized on (a) PAAm-PFPA, and (b) PFPA-silane surfaces.

SECTION 4

CONCLUSION

In summary, a polymer-based PFPA surface, PAAm-PFPA, has been developed for the covalent immobilization of nanomaterials, polymers, graphene and small molecules. This was accomplished by a step-wise procedure including 1) treating piranha-cleaned silicon wafers with PFPA-silane, 2) coating and UV irradiation to immobilize PAAm, and 3) reacting with PFPA-NHS. The generated surfaces were characterized by contact angle goniometry, ellipsometry, and IR. The PAAm surface was further characterized by determining the amine density on the surface. An alternative approach to generate PAAm-PFPA surface was also investigated where PAAm was coupled to epoxy-functionalized wafers. In this case, however, very small amount of PFPA was conjugated as indicated by ellipsometry and IR. Our explanation was that the amino groups on PAAs were mostly consumed by the surface epoxy groups leaving very little to react with PFPA-NHS. This method was therefore not used in the subsequent immobilization studies.

The PAAm-PFPA surface has been successfully employed to immobilize polymers, nanoparticles, graphene and small molecules. In the cases of nanoparticles, graphene and Man2, much higher immobilization efficiencies were obtained on the PAAm-PFPA surface as compared to the PFPA-silane surface. The PAAm-PFPA surface owes its advantage to the PAAm polymer, which provides a softer surface than the SAM surface of PFPA-silane. For solid materials like nanoparticles and

grapheme, the soft surface provides a closer and more conformal contact. The rougher PAAm surface also increases the contact areas with the coated molecules and materials facilitating the solid-state coupling reaction.

REFERENCES

- (1) Luzinov, I.; Minko, S.; Tsukruk, V. V.: Adaptive and responsive surfaces through controlled reorganization of interfacial polymer layers. *Prog. Polym. Sci.* **2004**, 29, 635-698.
- (2) Balamurugan, S.; Obubuafo, A.; Soper, S. A.; Spivak, D. A.: Surface immobilization methods for aptamer diagnostic applications. *Anal. Bioanal. Chem.* **2008**, 390, 1009-1021.
- (3) Craighead, H. G.: Nanoelectromechanical systems. *Science* **2000**, 290, 1532-1535.
- (4) Eda, G.; Fanchini, G.; Chhowalla, M.: Large-area ultrathin films of reduced graphene oxide as a transparent and flexible electronic material. *Nature Nanotechnology* **2008**, 3, 270-274.
- (5) Massad-Ivanir, N.; Shtenberg, G.; Zeidman, T.; Segal, E.: Construction and Characterization of Porous SiO(2)/Hydrogel Hybrids as Optical Biosensors for Rapid Detection of Bacteria. *Adv. Funct. Mater.* **2010**, 20, 2269-2277.
- (6) Park, S.; Ruoff, R. S.: Chemical methods for the production of graphenes. *Nature Nanotechnology* **2009**, 4, 217-224.
- (7) Stewart, M. P.; Buriak, J. M.: Chemical and biological applications of porous silicon technology. *Adv. Mater.* **2000**, 12, 859-869.
- (8) Ulman, A.: Formation and structure of self-assembled monolayers. *Chem. Rev.* **1996**, 96, 1533-1554.
- (9) Veiseh, M.; Zareie, M. H.; Zhang, M. Q.: Highly selective protein patterning on gold-silicon substrates for biosensor applications. *Langmuir* **2002**, 18, 6671-6678.
- (10) Prakash, S.; Karacor, M. B.; Banerjee, S.: Surface modification in microsystems and nanosystems. *Surf. Sci. Rep.* **2009**, 64, 233-254.
- (11) Akamatsu, Y.; Tsushima, N.; Goto, T.; Hibi, K.: INFLUENCE OF SURFACE-ROUGHNESS SKEWNESS ON ROLLING-CONTACT FATIGUE LIFE. *Tribology Transactions* **1992**, 35, 745-750.
- (12) Chandrasekharan, R.; Zhang, L.; Ostroverkhov, V.; Prakash, S.; Wu, Y.; Shen, Y.-R.; Shannon, M. A.: High-temperature hydroxylation of alumina crystalline surfaces. *Surf. Sci.* **2008**, 602, 1466-1474.
- (13) Chen, Q.; Richardson, N. V.: Surface facetting induced by adsorbates. *Prog. Surf. Sci.* **2003**, 73, 59-77.
- (14) Revathi, N.; Prathap, P.; Reddy, K. T. R.: Synthesis and physical behaviour of In₂S₃ films. *Appl. Surf. Sci.* **2008**, 254, 5291-5298.
- (15) Saul, G.; Roberson, J. A.; Adair, A. M.: EFFECTS OF THERMAL TREATMENT ON AUSTENITIC GRAIN SIZE AND MECHANICAL PROPERTIES OF 18 PERCENT NI MARAGING STEELS. *Metallurgical Transactions* **1970**, 1, 383-&.
- (16) Singh, R. K.; FitzGerald, J. M.: Laser induced formation of micro-rough structures. *Nuclear Instruments & Methods in Physics Research Section B-Beam Interactions with Materials and Atoms* **1997**, 121, 363-366.

- (17) Wang, H.; Chen, W.; Madey, T. E.: Morphological evolution in oxygen-induced faceting of Re(12(3)-over-bar1). *Physical Review B* **2006**, 74.
- (18) Aswal, D. K.; Lenfant, S.; Guerin, D.; Yakhmi, J. V.; Vuillaume, D.: Self assembled monolayers on silicon for molecular electronics. *Anal. Chim. Acta* **2006**, 568, 84-108.
- (19) Chaki, N. K.; Vijayamohanan, K.: Self-assembled monolayers as a tunable platform for biosensor applications. *Biosens. Bioelectron.* **2002**, 17, 1-12.
- (20) Parikh, A. N.; Allara, D. L.; Azouz, I. B.; Rondelez, F.: AN INTRINSIC RELATIONSHIP BETWEEN MOLECULAR-STRUCTURE IN SELF-ASSEMBLED N-ALKYLSILOXANE MONOLAYERS AND DEPOSITION TEMPERATURE. *J. Phys. Chem.* **1994**, 98, 7577-7590.
- (21) Pignataro, B.; Licciardello, A.; Cataldo, S.; Marletta, G.: SPM and TOF-SIMS investigation of the physical and chemical modification induced by tip writing of self-assembled monolayers. *Materials Science & Engineering C-Biomimetic and Supramolecular Systems* **2003**, 23, 7-12.
- (22) Samanta, D.; Sarkar, A.: Immobilization of bio-macromolecules on self-assembled monolayers: methods and sensor applications. *Chem. Soc. Rev.* **2011**, 40, 2567-2592.
- (23) Schwartz, D. K.: Mechanisms and kinetics of self-assembled monolayer formation. *Annu. Rev. Phys. Chem.* **2001**, 52, 107-137.
- (24) Davis, F.; Higson, S. P. J.: Structured thin films as functional components within biosensors. *Biosens. Bioelectron.* **2005**, 21, 1-20.
- (25) Wasserman, S. R.; Tao, Y. T.; Whitesides, G. M.: STRUCTURE AND REACTIVITY OF ALKYLSILOXANE MONOLAYERS FORMED BY REACTION OF ALKYLTRICHLOROSILANES ON SILICON SUBSTRATES. *Langmuir* **1989**, 5, 1074-1087.
- (26) Haensch, C.; Hoeppener, S.; Schubert, U. S.: Chemical modification of self-assembled silane based monolayers by surface reactions. *Chem. Soc. Rev.* **2010**, 39, 2323-2334.
- (27) Chandekar, A.; Sengupta, S. K.; Whitten, J. E.: Thermal stability of thiol and silane monolayers: A comparative study. *Appl. Surf. Sci.* **2010**, 256, 2742-2749.
- (28) Liu, L. H.; Yan, M. D.: Perfluorophenyl Azides: New Applications in Surface Functionalization and Nanomaterial Synthesis. *Acc. Chem. Res.* **2010**, 43, 1434-1443.
- (29) Yan, M. D.; Bartlett, M. A.: Micro/nanowell arrays fabricated from covalently immobilized polymer thin films on a flat substrate. *Nano Lett.* **2002**, 2, 275-278.
- (30) Liu, L.; Yan, M.: A general approach to the covalent immobilization of single polymers. *Angewandte Chemie-International Edition* **2006**, 45, 6207-6210.
- (31) Liu, L.-H.; Dietsch, H.; Schurtenberger, P.; Yan, M.: Photoinitiated Coupling of Unmodified Monosaccharides to Iron Oxide Nanoparticles for Sensing Proteins and Bacteria. *Bioconjug. Chem.* **2009**, 20, 1349-1355.
- (32) Takuya Kubo, X. W., Qi Tong, and Mingdi Yan: Polymer-Based Photocoupling Agent for the Efficient Immobilization of Nanomaterials and Small Molecules. *Langmuir* **2011**, 27.

- (33) Liu, L.-H.; Yan, M.: Simple Method for the Covalent Immobilization of Graphene. *Nano Lett.* **2009**, *9*, 3375-3378.
- (34) Liu, L.-H.; Zorn, G.; Castner, D. G.; Solanki, R.; Lerner, M. M.; Yan, M.: A simple and scalable route to wafer-size patterned graphene. *J. Mater. Chem.* **2010**, *20*, 5041-5046.
- (35) Liu, L.-H.; Lerner, M. M.; Yan, M.: Derivatization of Pristine Graphene with Well-Defined Chemical Functionalities. *Nano Lett.* **2010**, *10*, 3754-3756.
- (36) Al-Bataineh, S. A.; Luginbuehl, R.; Textor, M.; Yan, M.: Covalent Immobilization of Antibacterial Furanones via Photochemical Activation of Perfluorophenylazide. *Langmuir* **2009**, *25*, 7432-7437.
- (37) Norberg, O.; Deng, L.; Yan, M.; Ramstrom, O.: Photo-Click Immobilization of Carbohydrates on Polymeric Surfaces-A Quick Method to Functionalize Surfaces for Biomolecular Recognition Studies. *Bioconjug. Chem.* **2009**, *20*, 2364-2370.
- (38) Wang, X.; Ramstrom, O.; Yan, M.: A photochemically initiated chemistry for coupling underivatized carbohydrates to gold nanoparticles. *J. Mater. Chem.* **2009**, *19*, 8944-8949.
- (39) Graupner, R. K.; Yan, M. D.: Theoretical model for photochemical or thermally activated immobilization of macromolecules. *Langmuir* **2004**, *20*, 8675-8680.
- (40) Keana, J. F. W.; Cai, S. X.: NEW REAGENTS FOR PHOTOAFFINITY-LABELING - SYNTHESIS AND PHOTOLYSIS OF FUNCTIONALIZED PERFLUOROPHENYL AZIDES. *J. Org. Chem.* **1990**, *55*, 3640-3647.
- (41) Yan, M. D.; Ren, J.: Covalent immobilization of ultrathin polymer films by thermal activation of perfluorophenyl azide. *Chem. Mater.* **2004**, *16*, 1627-1632.
- (42) Moon, J. H.; Kim, J. H.; Kim, K.; Kang, T. H.; Kim, B.; Kim, C. H.; Hahn, J. H.; Park, J. W.: Absolute surface density of the amine group of the aminosilylated thin layers: Ultraviolet-visible spectroscopy, second harmonic generation, and synchrotron-radiation photoelectron spectroscopy study. *Langmuir* **1997**, *13*, 4305-4310.
- (43) Stober, W.; Fink, A.; Bohn, E.: CONTROLLED GROWTH OF MONODISPERSE SILICA SPHERES IN MICRON SIZE RANGE. *J. Colloid Interface Sci.* **1968**, *26*, 62-&.
- (44) Green, D. L.; Lin, J. S.; Lam, Y. F.; Hu, M. Z. C.; Schaefer, D. W.; Harris, M. T.: Size, volume fraction, and nucleation of Stober silica nanoparticles. *J. Colloid Interface Sci.* **2003**, *266*, 346-358.
- (45) Liu, L.; Engelhard, M. H.; Yan, M.: Surface and interface control on photochemically initiated immobilization. *J. Am. Chem. Soc.* **2006**, *128*, 14067-14072.
- (46) Lieber, E.; Rao, C. N. R.; Chao, T. S.; Hoffman, C. W. W.: INFRARED SPECTRA OF ORGANIC AZIDES. *Anal. Chem.* **1957**, *29*, 916-918.
- (47) Moon, J. H.; Kim, J. H.; Hahn, J. H.; Park, J. P.: Absolute surface density of the amine group of the aminosilylated thin layers: UV-vis spectroscopy, ellipsometry, and second harmonic generation study. *Abstracts of Papers of the American Chemical Society* **1997**, *214*, 369-PHYS.

(48) Wang, H.; Zhang, Y.; Yuan, X.; Chen, Y.; Yan, M.: A Universal Protocol for Photochemical Covalent Immobilization of Intact Carbohydrates for the Preparation of Carbohydrate Microarrays. *Bioconjug. Chem.* **2011**, 22, 26-32.

(49) Wang, H.; Li, L.; Tong, Q.; Yan, M.: Evaluation of Photochemically Immobilized Poly(2-ethyl-2-oxazoline) Thin Films as Protein-Resistant Surfaces. *ACS applied materials & interfaces* **2011**, 3, 3463-71.